Evolution of the oxidation of V zigzag nanostructures on Si: prime conditions to reach uniform thermochromic VO_2(M) thin films

Francisco M. Morales[1,2,*], *Juan J. Jiménez*[1,2], *Nicolas Martin*[3], *Rodrigo Alcántara*[1,4], *Javier Navas*[1,4], *Rafael García*[1,2], *Antonio J. Santos*[1,2,*].

[1] IMEYMAT: Institute of Research on Electron Microscopy and Materials of the University of Cádiz, E-11510, Puerto Real, Spain.

[2] Department of Materials Science and Metallurgic Engineering, and Inorganic Chemistry, Faculty of Sciences, University of Cádiz, E-11510 Puerto Real, Spain.

[3] SUPMICROTECH, CNRS, Institut FEMTO-ST, F-25000 Besançon Cedex, France.

[4] Department of Physical Chemistry, Faculty of Sciences, University of Cádiz, E-11510 Puerto Real, Spain.

KEYWORDS: vanadium oxidation; vanadium dioxide synthesis; glancing angle deposition; flash lamp annealing; electron microscopy; Raman spectroscopy; Vis-NIR spectrophotometry; thermochromism; smart coatings.

ABSTRACT: This article reports on the oxidation of 100 nm-thick vanadium layers achieved by sputtering glancing-angle deposition on silicon, with opposite oblique columns creating a zigzag morphology, using a small overpressure continuous flow of air and an infrared lamps furnace. In addition, the study focuses on the stepwise investigation of the nanostructure and the layer's oxidation progress by electron microscopy, verifying a monotonic incorporation of oxygen with time, which results in a linear rise of the VO_x overlayer volumes. This characterization is correlated with Raman spectra fast collected in a wide wavelength range. In consequence, we claim a methodology based on the relative intensities of such Raman bands to track the kinetic dynamics of these systems, evidencing the participation of three main phases: VO_2(M) alone or mixed either with V or V_2O_5. For the optimum conditions, high-quality vanadium dioxide layers are achieved, attending to their nanostructure and outstanding optical response (over 90% of relative transmittance modulation at a wavelength of 3000 nm). Vis-NIR spectrophotometry and Raman spectroscopy, both at variable temperature, allow exploring the different thermochromic characteristics of the samples at different oxidation stages.

1. Introduction

Monoclinic (M) vanadium dioxide (VO_2) is receiving an increasing attention due to its thermochromic characteristics implying a reversible phase transition with temperature accompanied by abrupt changes not only at the structural level but on its optical, thermal, mechanical and electrical performances. Two types of platforms are being researched for this compound: Transparent substrates on the one side (i.e., glass, sapphire, quartz, ITO, polymers…) and opaque substrates on the other. The first group mainly focuses on maximizing optical and thermochromic performances in the regions coincident with the solar spectrum activity for smart windows (probably the most investigated application of this material), and other usages as in ultrafast optical switches. When the visible light transmission is not an important issue, many other uses are envisaged for VO_2(M), with silicon substrates often being the most preferred templates, since there is a vast know-how on its industrial manufacture, its availability as a large-scale support and, in many cases, its electronics or photonics characteristics give additional advantages to the foreseen VO_2-based devices. In addition, the bistability and width of the implicit hysteresis of different dioxide systems have been highlighted as key features to improve the reproducibility of operational modes in thermotronics (switching, memory, logical operations, etc.)[1]. Some recent examples of applications of monoclinic VO_2 layers on Si platforms are optical memories[2], smart radiators[3], electrical switches and sensors[4–8], optical modulators, limiters or switches[9,10] or infrared photodetectors[11].

On the other hand, the dioxide is not the easiest vanadium oxide to synthesize. Due to the complex chemistry of vanadium, mainly promoted by its numerous available valence states, there are multiple stoichiometries and/or polymorphs that are more thermodynamically favorable. Therefore, only a constricted combination of reaction conditions allows achieving pure monoclinic VO_2 by different strategies, which comprise the reduction of V_2O_5, the oxidation of V, or the direct deposition of this dioxide, often combined with further annealing in vacuum or other controlled atmospheres. The challenging approaches to reach high-quality VO_2 coatings mostly involve complex or expensive methods (hydrothermal or chemical routes, sol-gel, electron-beam evaporation, pulsed-laser or chemical-vapor depositions…) that employ high vacuum, special reactive, multiple steps with long processing times, very small substrates, etc. Besides the wafer-scale growth of VO_2 on sapphire[12], there is a lack of methods to reach large-scale VO_2 surfaces on silicon, and we believe that the physical vapor deposition is a feasible, relatively simple, and low-cost way to reach industrial scalability. In this context, our group has been developing and improving an original and effective two-step approach to attain VO_2(M)/Si: In a first step, porous films of V nanostructures are sputtered by GLancing Angle Deposition (GLAD) and later, they are submitted to a fast but finely controlled thermal treatment in air atmosphere[13]. Based on this patented methodology of oxidation to achieve VO_2 in open tube reactors, of either free-standing V powders[14] or thin films of slanted V columns on Si[15] or glass[16], we have used this time, for the purpose of reproducibility, scalability and simplicity, a precursor of two sublayers of opposite oblique V nanocolumns forming a film on silicon, to be annealed in a continuous flow of air using heating lamps, and attain high-quality VO_2 coatings with exceptional optical performances. By tracking the oxidation stages associated to different reaction times, the optimal conditions for VO_2(M) synthesis can be found, allowing to establish correspondences between grains nanostructure and topography with the right bands in Raman spectra as well as with the resulting optical and thermochromic features.

2. Materials and Methods

Layers of GLAD vanadium nanocolums (one zigzag period) were deposited in a home-made magnetron sputtering chamber at angles of 85º on Si, with the same conditions to those reported elsewhere[13,15]. A MILA 5000 rapid thermal annealing system (from ULVAC GmbH), an inner continuous flow of 10 l/min of compressed air, and similar heating (40ºC/s) and cooling (-10ºC/s) ramps than those used for our previous trials on silicon, were chosen to oxidize, at a moderate temperature of 475ºC, a group of the described V-GLAD samples. These changes were motivated since (i) the zigzag geometry provides a more balanced gradient of porosity to the V-GLAD film by compensating the directional preferred shadowing effects of nanocolums, making them more homogeneous; (ii) infrared lamps allow to automatize the required high heating rates that were previously manually achieved by trained operators in a resistance furnace reactor at the same time while ensuring a larger uniform reaction surface till 20mm x 20mm; and (iii) the small but continuous air overpressure avoids the exhaustion of O_2 in the surrounding oxidative atmosphere, that might happen in calm air into open tubes. The specimens are named with the number of seconds that they were oxidized in the plateau of higher temperature.

The samples were studied by Scanning Electron Microscopy (SEM) and prepared for Transmission Electron Microscopy (TEM) by Focused-Ion Beams (FIB) in a Thermo Scientific Scios 2 DualBeam equipment. TEM experiments were carried out in a FEI Talos F200X system. Raman spectra were acquired in a LabRAM HR Evolution (Horiba Scientific) microscope, using a 532 nm excitation laser source, 20s of integration time, 10 averaged spectra, 10% of neutral filter power, x100 objective lens and a measurement wavenumber interval of 100–900 cm^{-1}. In order to compare the 612 cm^{-1} exclusive band of VO_2 at variable temperatures, a non-focalized 80 microns spot of a 473 nm laser wavelength was used to scan the 540–680 cm^{-1} interval, using

100% of neutral filter, 30s of integration time, 10 averaged spectra and x50 objective lens. The thermochromic optical behaviors of the prepared monoclinic VO_2-based films were determined by transmittance spectroscopy using a PerkinElmer Lambda 900 UV/VIS/NIR Spectrometer equipped with a THMS600 Linkam stage for temperature control. UV-Vis-NIR spectra were recorded in the wavelength range of 180–3300 nm at 25 and 100ºC. For the monitoring of the thermally induced phase transition, the transmittance at λ=3000 nm was observed in controlled rates of 5ºC/min for heating and -1ºC/min for cooling.

3. Results and discussion

There is a clear evolution of the nanostructures formed on the surface and along the layers upon oxidation, as confirmed by a rapid sight of **Figure 1**. This illustrates pairs of plain-view SEM (PVSEM: above) and cross-section TEM (XTEM: bellow) micrographs for the same samples. Note that the zigzag structure is evidenced for the less oxidized layers when visualized perpendicularly to the sputtering atomic flux (TEM of 1s and 5s) and their topographic characteristics are proper of the GLAD structure (see the SEM of the non-oxidized 0s sample to prove this), but a small cover of oxidized vanadium starts to be visible over them. Nevertheless, a top layer of vanadium oxide grains forms and seals more clearly the V in the process range from 30 to 150 s, while the underneath layer is being more and more consumed at the cost of new VO_x grains generation and coarsening. This demonstrates that, despite using a different reaction system (flash lamp heating), oxidation progresses in a similar way to our previous studies[15], i.e., from the surface of the coating towards the interface with the substrate. In the SEM series from 30 to 240s, grains are equiaxial and have an increasing diameter with time from units to tens of nanometers, till they coalesce, and later start to lose their roundness and turn to be more and more textured, while growing, at the 270 to 520s series. It is also observed that the development of such nanostructures lead to the appearance of sizeable intergranular voids. A fully corresponding picture of the PVSEM images is found in the associated XTEM micrographs.

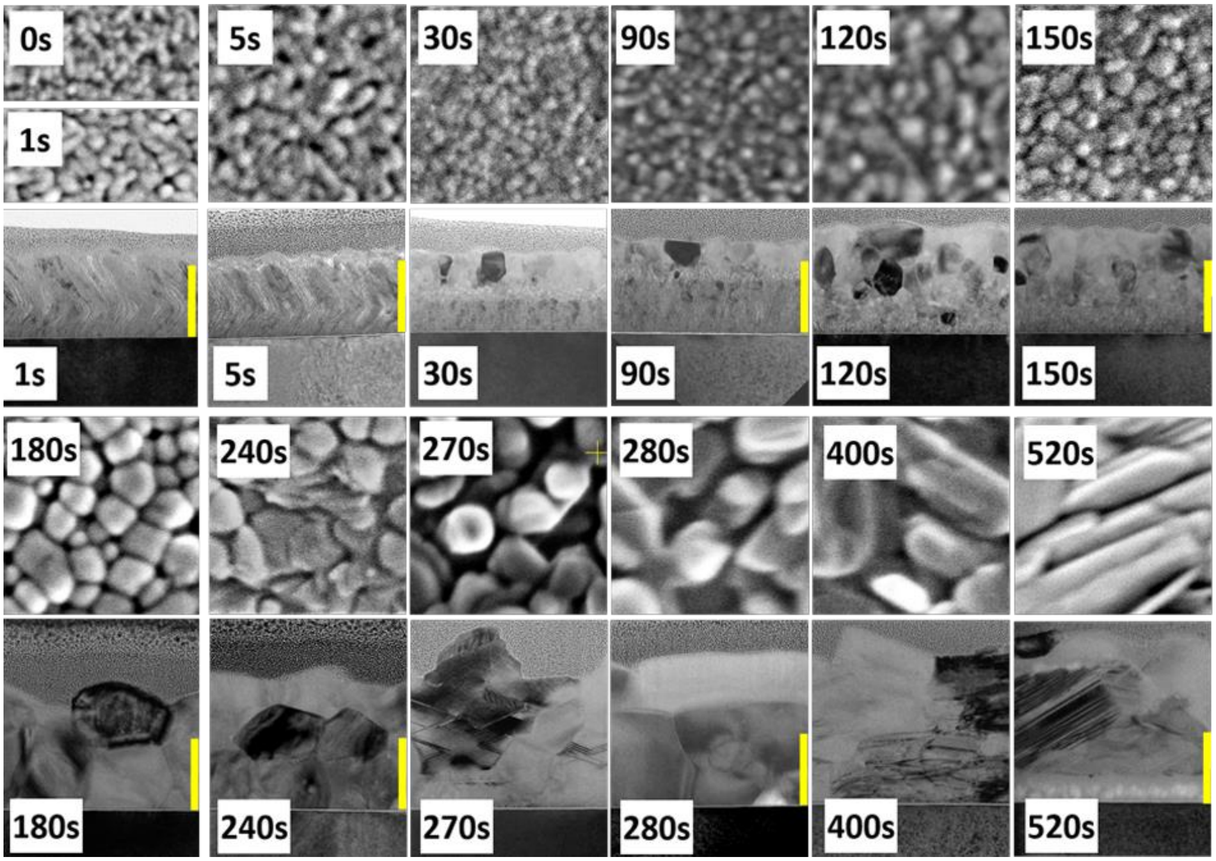

Figure 1. Top view SEM pictures of 500nm side, and lateral TEM images with yellow bars of 100 nm.

Furthermore, high-resolution and selected-area diffraction experiments were conducted for most of these TEM preparations in singular regions. The buried layers, when present (1 to 150 s), apparently from metallic V, are partially amorphous and present oxygen diffusion hints from the beginning (from 1s), and their porosity is fully filled soon with trace crystalline nanodomains (from 5s). In the top sublayers, where grains are always crystalline, basically VO_2(M) is found from 30 to 240 s. Although other species as V_6O_{13} and V_2O_3 were not found, they are not disregarded in residual amounts, considering previous studies[13]. In addition, from 240 to 520 s, V_2O_5 polygonal grains often containing planar defects, start to be more and more predominant while VO_2 is diminishing. The kinetics of this oxidation can be estimated when observing how the thickness of the sum of reacted sublayers increases. **Figure 2(a)** shows that there is a trend in the measure of this characteristic with respect to the oxidation time, that can be fitted linearly with R^2=0.95. This agrees with ancient studies that claim that oxidation of V is linear or parabolic and that VO_2 and V_2O_5 are the dominant developed phases[17]. **Figures 2(b)** and **(c)** show overview XTEM micrographs of samples 1s and 180s to demonstrate their high homogeneities and thickness invariability. **Figure 2(d)** displays a panoramic PVSEM of the 180s sample on the same purpose, where a regular topography of pseudo-spherical grains proper of equiaxial nanostructures are evident for a polycrystalline VO_2(M) coating.

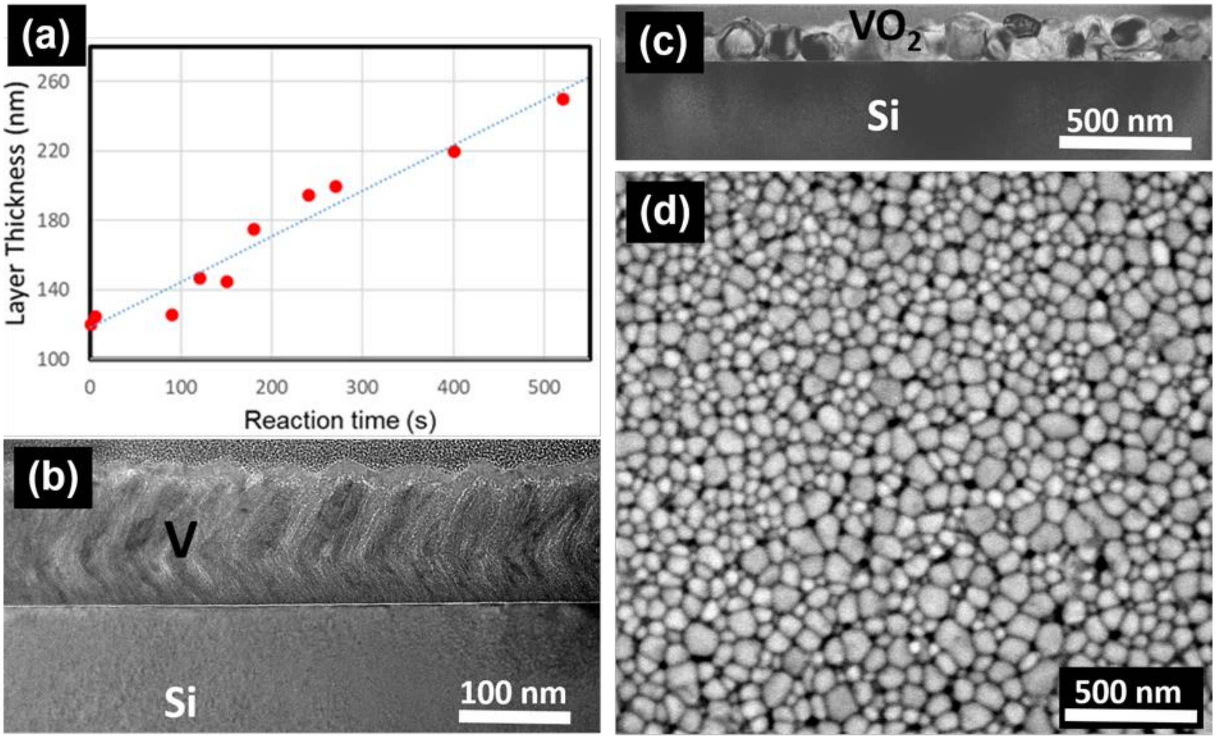

Figure 2. (a) Plot of the overlayer thickness with respect to the reaction time; (b) XTEM micrograph of sample 1s; (c) XTEM micrograph of sample 180s; (d) PVSEM image of sample 180s.

This demonstrates that the originally porous vanadium boomerang-like nanostructure (**Figure 2(b)**) is an efficient format for a gradual reaction due to its high surface-to-volume ratio. However, the fully consumed V is also able to keep on incorporating O with a similar velocity when vanadium dioxide is present till it collapses to the pentoxide phase with the maximum possible content of oxygen. This is certainly a cleaner scenario than the progress of freestanding or supported V nanostructures reactivity in open air[14,18], which demonstrated the appearance of additional phases different to VO_2 and V_2O_5 (i. e. $V_{16}O_3$, VO, V_2O_3, V_6O_{13}), and even a competence of oxidative and reductive effects for the nanoparticle arrangements. Indeed, in our recently reported method to oxidize V-GLAD slanted single columns in calm air into an open-tube inside a SiC resistance oven, and specifically for 100 nm films, the best sample in terms of higher VO_2 content was achieved at 475ºC for 60s[13]. By using the same heating and cooling rates, for the present conditions, the time of permanence must be kept thrice than the previous trials to reach the maximum content of VO_2, but note that this is still a remarkable short processing time with respect the rest of attempts on the same purpose[19,20]. The hypothesis to explain this slower reaction is that the porous V zigzag is slightly more sealed than the V single-columns opener structure. Nevertheless, as mentioned, there are intrinsic benefits in this new procedure, as better thickness stability, bigger processed areas, and operation simplicity.

These findings found a strong correlation with the Raman spectroscopy tracking of the same samples (**Figure 3**). In order to follow the reactions, step by step, the height of the exclusive VO_2(M) band at 223 cm^{-1} was normalized (to unity) for all spectra. One second of oxidation provides a noisy signal and a clearer band linked to the substrate, but the Si associated band intensity increases gradually up to very exaggerated, from the moment that VO_2(M) clearly appears (5s), till firstly vanadium is fully spent (150–180s), and later a V_2O_5 minority starts to appear (180–260s). This is explained by the fact that the film becomes increasingly transparent (the pentoxide is more transparent to light than the dioxide at the laser wavelength), with more photons reaching the substrate. However, it must also be considered that as oxidation progresses, it has also been shown that the overall thickness of the coating increases, so that the increase in this signal is not entirely proportional to oxidation progress (the greater the thickness, the lower the signal from the substrate). Thus, the use of this signal to normalize a spectrum is not recommended. As can be seen, between 5–150 s, VO_2(M) Raman bands are observed exclusively, which become increasingly more intense. In agreement with the XTEM observations, this would be associated with a progressive increase in the VO_2 volumes as the remaining reacting V (without Raman signal) buried material is consumed. The onset indicating that the pentoxide starts to dominate more and more in its relative amount with respect to the dioxide is marked when fingerprints of Si (521 cm^{-1}) and the most intense V_2O_5 band (144 cm^{-1}) that coincides in position with a weak (less than unit) VO_2(M) band, firstly equalize and later progress together from one of two orders of magnitude higher than the VO_2(M) reference band. In conclusion, the early appearance of V_2O_5 dominant signal (see two measurements of the 180s in different locations) marks the moment when VO_2(M) is in its maximum amount and only can progress to other phases by being consumed, as subsequent optical measurements also prove.

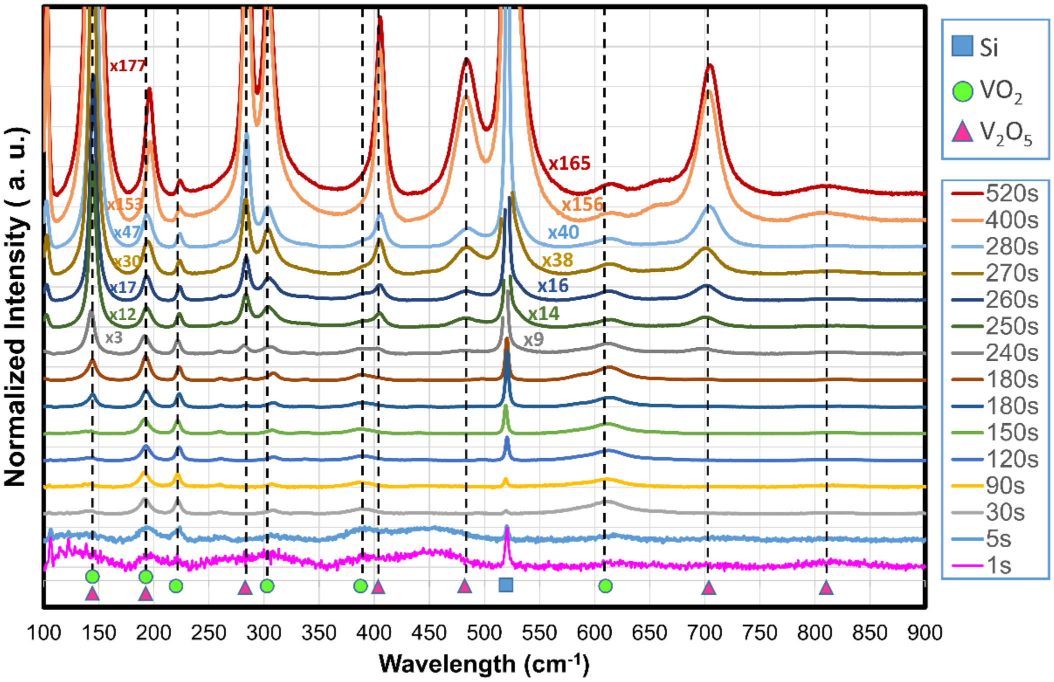

Figure 3. Raman spectra of samples useful for tracking the oxidation of V zigzag coatings on Si.

All the above suggests that the stronger thermochromic behavior (this means the maximum content of monoclinic VO_2) would be achieved when traces of V_2O_5 are present (in the 180s sample the more intense pentoxide band is in the same level than normalized dioxide band). It should also be highlighted that many bands of the dioxide compound are concurrent with those of other vanadium oxides, for example, those at 144 and 193 cm^{-1} are coincident with bands of V_2O_5[21]. In addition, the other VO_2 fingerprint band at 612 cm^{-1} was registered at different temperatures for specimen 180s, as shown in **Figure 4(a)** and **(b)** for the heating and cooling cycles, respectively. The intensity of this peak showed to be principal so it is the most appropriate for signal comparisons in order to plot the thermochromic phase transition[22]. The integral values of these Raman bands were represented and fitted to sigmoidal lines in **Figure 4(c)** showing the typical $VO_2(M)$ associated hysteresis, while the derivatives of these lines (inset in this figure) show the exact transition temperatures for heating ($T_{c(H)}$=68ºC) and cooling ($T_{c(C)}$=44ºC), which are indeed typical of pure $VO_2(M)$. In addition, the difference of these T_c values indicates the structural (Raman) hysteresis width of W_H=24ºC.

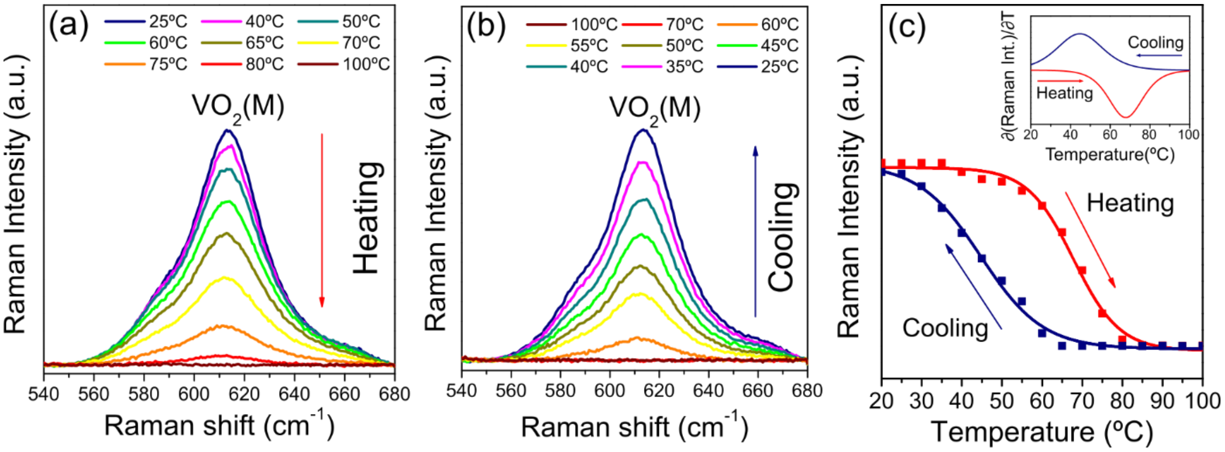

Figure 4. Raman spectra recorded for sample 180s at multiple temperatures between 25 and 100 °C during consecutive (a) heating and(b) cooling cycles. (c) Thermal evolution of the intensity of the VO_2(M) Raman band at 612 cm^{-1} during heating (red) and cooling (blue) cycles. The inset shows the derivative of each kinetic thermochromic cycle (the derivative of the cooling is plotted in absolute values).

The fact that 180s is the optimal specimen is also demonstrated by variable temperature Vis-NIR transmittance measurements. **Figure 5(a)** shows the transmittance spectra of some specimens selected with the purpose of displaying distinctive behaviors at temperatures below and above the switching one, in addition to their kinetics plots of transmittance levels when varying temperatures (consecutive heating and cooling cycles) at a fixed wavelength of 3000 nm, which are presented in **Figure 5(b)**.

Note that at any temperature the Si is opaque till about 1 µm, and over this value, it abruptly should let almost 50% of radiation pass through[22]. From the analysis of **Figure 5**, it is concluded that while samples annealed less than 180s present a near-zero transmittance at 100ºC, which could mean that either the only optically active phase is VO_2(R) or that the film is still highly reflective due to unreacted V, the transmittances at 25ºC above 1 μm suddenly stays in a relatively constant value that progressively increases as the oxidation time is higher. For 180s of optimal oxidation (in terms of VO_2 yield), the absolute NIR thermal modulation reaches more than 40% as those reported for high-quality VO_2 layers on Si[20]. This is because the quantity of dioxide maximizes at the cost of V consumption and lets the system transmit in a similar way than substrates. On the contrary, when V metal forms part of the mix (i.e., 30s and 120s), an additional blockage of the transmittance at the lower temperature occurs beyond the base effect already imposed by Si. For this reason, the less oxidized sample shows a low transmittance, and the middle oxidized one shows an intermediate transmittance. Obviously, this event negatively affects the thermal modulation capacity of the coatings in the NIR (lower VO_2(M) yields), which does not exceed 7 and 25%, respectively.

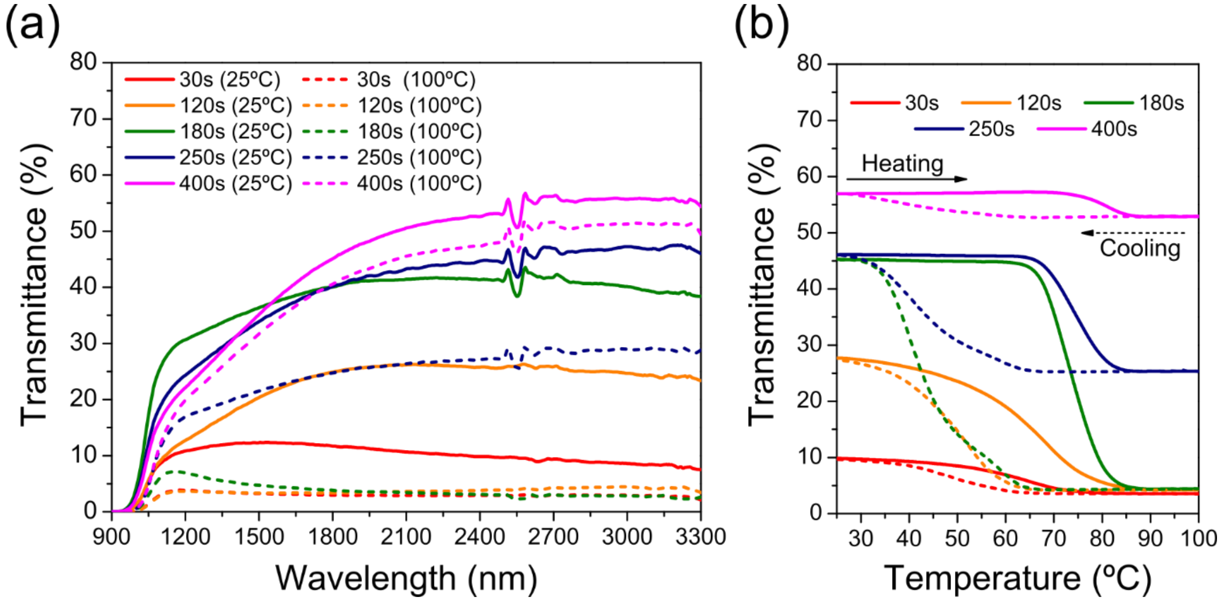

Figure 5. Vis-NIR optical measurements performed on 30s, 120s, 180s, 250s, and 400s samples. (a) Transmittance spectra recorded at 25ºC (solid lines) and 100ºC (dashed lines) for selected samples. (b) Thermal evolution of the optical transmittance at 3000 nm recorded during consecutive heating (solid lines) and cooling (dashed lines) cycles for selected samples.

For overoxidized coatings, when a minority or majority of V_2O_5 is present together with the rest of VO_2, respectively, a more remarkable (250s) or slight (400s) thermochromic effect is still appreciable, which in turn translates into progressive increases in NIR transmittances at high and low temperatures with respect to those observed in VO_2(+V) coatings. The cause of this transmittance intensification, sometimes even higher than that of the bare silicon substrate, can be associated with the combined effect of the higher intrinsic transparency of the pentoxide phase compared to that of the VO_2(R), as well as the antireflective effect that it stimulates on the Si surface, due to the particular plate-like and open (voided) structures formed on these latter samples promoting a high overall porosity[23]. **Table 1** collects the maximum and minimum transmittance percentages of each sample for 3000 nm at the higher and lower temperature, respectively, together with the value of relative transmittance of the VO_2-based coatings, which is indicative of their qualities and performances. Note that the relative NIR modulation of sample 180s is over 90%, and this is an outstanding value indicating the dioxide purity, a value that we had not reached in our previous studies and not many authors claimed.

It is also remarkable the fact that the VO_2(M) phase transition temperatures vary as a function of the oxidation time, and this can be concluded visually in **Figure 5(b)**, but a derivative analysis of the main features of the thermochromic hysteresis loops, similar to that shown in **Figure 4(c)**, allows to quantify these differences (presented in **Table 1**). Note that some of these peaks at heating or cooling better fitted to a double Gaussian, and the differences of the T_c values, let also calculate the hysteresis widths (W_H). It is possible to conclude that as V layers are more and more oxidized, values of T_c increase at heating and decrease at cooling, having the consequence that W_H dimensions amplify with greater reaction times. The hysteresis width can be a key feature for some applications, for example, in optical storage-type devices, which require the widest possible hysteresis (>15ºC) to operate reliably[24]. Likewise, longer oxidation times lead to increasingly asymmetric hysteresis loops, which are especially reflected in the cooling stage. As can be seen in **Figure 5(b)**, the higher the VO_2 content, the sharper the transition during the heating. However, it has been reported that structural and/or compositional heterogeneities can act by slowing down the VO_2(R) to VO_2(M) transition, resulting in the development of wide and asymmetric hysteresis loops[16,25–27]. These assumptions would explain the observed thermochromic behaviors in line with electron microscopy and Raman spectroscopy findings. Comparing the values of T_c and W_H extracted from the Raman and transmittance hysteresis of sample 180s, it seems that having a similar range of temperature activity, the optical intermittence is about 10ºC wider than the structural phase change one. Moreover, the optical MIT (metal to insulator) transition is activated (on heating) about 6ºC above the structural one, which is fine in agreement with the observation of this effect in earlier studies[13].

Table 1. Main features of the thermochromic hysteresis loops shown in Figure 5: T_{max}, and T_{min} denote the λ=3000 nm transmittances at 25ºC and 100ºC; ΔT_{rel} is the relative decrease in the transmittance upon the transition at that wavelength; $T_{c(H1)}$ and $T_{c(H2)}$ denote the temperatures of the MIT for heating; $T_{c(C1)}$ and $T_{c(C2)}$ indicate the temperatures of the MIT for cooling; W_{H1} and W_{H2} are the hysteresis loop widths given by $T_{c(H1)} - T_{c(C1)}$ and $T_{c(H2)} - T_{c(C2)}$, respectively. Accuracy of the temperature and transmittance values are ±0.5°C and ± 0.1%, respectively.

Sample	**T_{max} (%)**	**T_{min} (%)**	**ΔT_{rel} (%)**	**T_c (ºC) Heating** *Main peak		**T_c (ºC) Cooling** *Main peak		**W_H (ºC)**	
				H1	**H2**	**C1**	**C2**	**1**	**2**
30s	9.9	3.5	64.6	53	65*	49		4	16
120s	27.7	4.2	84.8	57	68*	53	46*	4	22
180s	45.3	4.4	90.3	74		56	41*	18	33
250s	46.1	25.3	45.1	74		58	41*	16	33
400s	57.0	52.9	7.2	75	81*	57	37*	18	44

4. Conclusions

A porous 100 nm-thick film of V nano-boomerangs on silicon achieved by a two-step glancing angle sputtering deposition turns into a 50% thicker compact polycrystalline film of coalesced round monoclinic VO_2 grains when exposed to a compressed air current at 475ºC for 3 minutes after fast heating with infrared lamps and further cooling with air flow and switched off lamps.

This almost pure vanadium dioxide layer shows outstanding optical properties when the transmittances are measured at different temperatures, consisting in a relative infrared modulation (at 3000 nm) over 90%, near-zero NIR transmittances at temperatures above its T_c=74ºC at heating and T_c=41ºC at cooling, and an asymmetric hysteresis loop with a maximum width of 33ºC. Many precursor V-OAD/Si specimens were heat treated at the same temperature and different times for tracing the kinetics of oxidation. The progress of nanostructures shown by SEM/TEM microscopies and of Raman spectroscopy bands finds such a good agreement, that both follow-ups can be used to decide the best moment for achieving the maximum quantity of VO_2(M): the beginning of lack of roundness in the previously coarsened grains and the faint appearance of V_2O_5 peaks.

AUTHOR INFORMATION

Corresponding Author

*Email: fmiguel.morales@uca.es; antonio.santos@uca.es

Author Contributions

The manuscript was written through contributions of all authors. All authors have given approval to the final version of the manuscript.

Funding Sources

This work was supported by the Spanish State R&D projects (Retos y Generación de Conocimiento) with references PID2020–114418RBI00 and PID2023-150975OB-I00. This work was partly supported by the French RENATECH network, FEMTO-ST technological facility, by the Region Bourgogne-Franche-Comté and by EIPHI Graduate School (Contract “ANR–17–EURE–0002”).

ACKNOWLEDGMENT

A. J. Santos would like to thank the University of Cádiz and the Spanish Ministerio de Universidades for the concession of a “Margarita Salas” postdoctoral fellowship funded by the European Union - NextGenerationEU (2021-067#9663/PN/MS-RECUAL/CD). University of Cádiz and IMEYMAT are also acknowledged by financing the mutual facilities available at the UCA R&D Central Services (SC-ICYT) and the UCA project reference “PUENTE PR2022-027”. J. J. Jiménez also acknowledge Spanish Ministry of Science and Innovation for the granting of a postdoctoral contract within the framework of the project Ref. PID2020–114418RBI00.

REFERENCES

(1) Sahoo, S.; Juneau-Fecteau, A.; Lamirand, A.; Pierron, V.; Mechin, L.; Frechette, L.; Vilquin, B. Integration of VO_2 on Silicon for Thermotronic Applications. In *JMC 2022 (Journées de la matière condensée), Société française de physique (SFP),*; Lyon, France, 2022.

(2) Jung, Y.; Han, H.; Sharma, A.; Jeong, J.; Parkin, S. S. P.; Poon, J. K. S. Integrated Hybrid VO_2–Silicon Optical Memory. *ACS Photonics* **2022**, *9* (1), 217–223.

(3) Benkahoul, M.; Chaker, M.; Margot, J.; Haddad, E.; Kruzelecky, R.; Wong, B.; Jamroz, W.; Poinas, P. Thermochromic VO_2 Film Deposited on Al with Tunable Thermal Emissivity for Space Applications. *Sol. Energy Mater. Sol. Cells* **2011**, *95* (12), 3504–3508.

(4) Roul, B.; Singh, D. K.; Pant, R.; Chowdhury, A. M.; Nanda, K. K.; Krupanidhi, S. B. Electrical Transport Modulation of VO_2/Si(111) Heterojunction by Engineering Interfacial Barrier Height. *J. Appl. Phys.* **2021**, *129*, 244502.

(5) Annadi, A.; Bohra, M.; Singh, V. Modulations in Electrical Properties of Sputter Deposited Vanadium Oxide Thin Films: Implication for Electronic Device Applications. *Thin Solid Films* **2022**, *758*, 139451.

(6) Murtagh, O.; Walls, B.; Shvets, I. V. Controlling the Resistive Switching Hysteresis in VO_2 thin Films via Application of Pulsed Voltage. *Appl. Phys. Lett.* **2020**, *117*, 063501.

(7) Yang, Z.; Ko, C.; Ramanathan, S. Oxide Electronics Utilizing Ultrafast Metal-Insulator Transitions. *Annu. Rev. Mater. Res.* **2011**, *41*, 337–367.

(8) Rana, A.; Li, C.; Koster, G.; Hilgenkamp, H. Resistive Switching Studies in VO_2 Thin Films. *Sci. Rep.* **2020**, *10*, 3293.

(9) Parra, J.; Navarro-Arenas, J.; Menghini, M.; Recaman, M.; Pierre-Locquet, J.; Sanchis, P. Low-Threshold Power and Tunable Integrated Optical Limiter Based on an Ultracompact VO_2/Si Waveguide. *APL Photonics* **2021**, *6*, 121301.

(10) Qi, J.; Zhang, D.; He, Q.; Zeng, L.; Liu, Y.; Wang, Z.; Zhong, A.; Cai, X.; Ye, F.; Fan, P. Independent Regulation of Electrical Properties of VO_2 for Low Threshold Voltage Electro-Optic Switch Applications. *Sensors Actuators A Phys.* **2022**, *335*, 113394.

(11) Selman, A. M.; Kadhim, M. J. Fabrication of High Sensitivity and Fast Response IR Photodetector Based on VO_2 Nanocrystalline Thin Films Prepared on the Silicon Substrate. *Opt. Mater. (Amst).* **2022**, *131*, 112664.

(12) Zhang, H. T.; Zhang, L.; Mukherjee, D.; Zheng, Y. X.; Haislmaier, R. C.; Alem, N.; Engel-Herbert, R. Wafer-Scale Growth of VO_2 Thin Films Using a Combinatorial Approach. *Nat. Commun.* **2015**, *6*, 8475.

(13) Santos, A. J.; Martin, N.; Jiménez, J. J.; Alcántara, R.; Margueron, S.; Casas-Acuña, A.; García, R.; Morales, F. M. Facile Fabrication of High-Performance Thermochromic VO_2-Based Films on Si for Application in Phase-Change Devices. *Chem. Mater.* **2023**, *35* (11), 4435–4448.

(14) Santos, A. J.; Escanciano, M.; Suárez-Llorens, A.; Pilar Yeste, M.; Morales, F. M. A Novel Route for the Easy Production of Thermochromic VO_2 Nanoparticles. *Chem. - A Eur. J.* **2021**, *27* (67), 16662–16669.

(15) Santos, A. J.; Lacroix, B.; Domínguez, M.; García, R.; Martin, N.; Morales, F. M. Controlled Grain-Size Thermochromic VO_2 Coatings by the Fast Oxidation of Sputtered Vanadium or Vanadium Oxide Films Deposited at Glancing Angles. *Surf. Interfaces* **2021**, *27*, 101581.

(16) Santos, A. J.; Martin, N.; Outón, J.; Blanco, E.; García, R.; Morales, F. M. A Simple Two-Step Approach to the Fabrication of VO_2-Based Coatings with Unique Thermochromic Features for Energy-Efficient Smart Glazing. *Energy Build.* **2023**, *285*, 112892.

(17) Mukherjee, A.; Wach, S. P. Kinetics of the Oxidation of Vanadium in the Temperature Range 350–950°C. *J. Less-Common Met.* **1983**, *92*, 289–300.

(18) Morales, F. M.; Escanciano, M.; Yeste, M. del P.; Santos, A. J. Reactivity of Vanadium Nanoparticles with Oxygen and Tungsten. *Nanomaterials* **2022**, *12*, 1471.

(19) Choi, H.; Lee, W.; Lim, J.; Shin, H.; Kumar, M.; Seo, H. Interface and Bulk Engineering of VO_2 Thin Film Deposited on Si for Multi-Level Metal-to-Insulator Transitions. *Appl. Surf. Sci.* **2023**, *611*, 155648.

(20) Zhang, C.; Koughia, C.; Li, Y.; Cui, X.; Ye, F.; Shiri, S.; Sanayei, M.; Wen, S.; Yang, Q.; Kasap, S. Near-Zero IR Transmission of VO_2 Thin Films Deposited on Si Substrate. *Appl. Surf. Sci.* **2018**, *440*, 415–420.

(21) Dzhagan, V. M.; Valakh, M. Y.; Isaieva, O. F.; Yukhymchuk, V. O.; Stadnik, O. A.; Gudymenko, O. Y.; Lytvyn, P. M.; Kulbachynskyi, O. A.; Yefanov, V. S.; Romanyuk, B. M.; Melnik, V.P.; Lashkaryov, V. Raman Fingerprints of Different Vanadium Oxides as Impurity Phases in VO_2 Films. *Opt. Mater. (Amst).* **2024**, *148*, 114894.

(22) Zhang, C.; Koughia, C.; Günes, O.; Cui, X.; Wen, S.; Wong, R.; Yang, Q.; Kasap, S. Synthesis , Structure and Optical Properties of High-Quality VO_2 Thin Films Grown on Silicon, Quartz and Sapphire Substrates by High Temperature Magnetron Sputtering : Properties through the Transition Temperature. *J. Alloy. Compd. J.* **2020**, *848*, 156323.

(23) Vi, J.; Janulevi, A.; Maneikis, A.; Matulaitien, I.; Selskis, A.; Stanionyt, S. Antireflection TiO_2 Coatings on Textured Surface Grown by HiPIMS. *Thin Solid Films* **2017**, *628*, 190–195.

(24) Zhang, H.; Wu, Z.; He, Q.; Jiang, Y. Preparation and Investigation of Sputtered Vanadium Dioxide Films with Large Phase-Transition Hysteresis Loops. *Appl. Surf. Sci.* **2013**, *277*, 218–222.

(25) Santos, A. J.; Martin, N.; Jiménez, J. J.; García, R.; Morales, F. M. Enhancing Luminous Transmittance and Hysteresis Width of VO_2-Based Thermochromic Coatings by Combining GLAD and RGPP Approaches. *Constr. Build. Mater.* **2024**, *419*, 135472.

(26) Gao, Y.; Luo, H.; Zhang, Z.; Kang, L. Nanoceramic VO_2 Thermochromic Smart Glass : A Review on Progress in Solution Processing. *Nano Energy* **2012**, *1*, 221–246.

(27) Currie, M.; Wheeler, V. D.; Downey, B.; Nepal, N.; Qadri, S. B.; Wollmershauser, J. A.; Avila, J.; Nyakiti, L. Asymmetric Hysteresis in Vanadium Dioxide Thin Films. *Opt. Mater. Express* **2019**, *9*, 3717–3728.